Autonomous Cascaded Photovoltaic System

Ahmed A. A. Hafez[1] Daniel Montesions-Miracle[2] Antoni Sudria-Andreu[2]
[1]Electrical Engineering Department, Faculty of Engineering, Assiut University, Assiut, Egypt, PO 71516 elhafez@aun.edu.eg
[2]Centre d'Innovació Tecnològica en Convertidors Estàtics i Accionaments (CITCEA-UPC), Departament d'Enginyeria Elèctrica, Universitat Politècnica de Catalunya.ETS d'Enginyeria Industrial de Barcelona, Av. Diagonal, 647, Pl. 2. 08028 Barcelona, Spain

***Abstract*- This paper proposes multi-level PV system; three PV generators each coupled to a buck cell. Each PV-generator-buck-converter channel is controlled such that maximum power is captured independently under different irradiation and temperature levels. The system operation under normal/abnormal conditions is investigated by thoroughly mathematical and simulation work.**

I. INTRODUCTION

The Photovoltaic (PV) systems are expected to play a promising role in fulfilling the future electricity requirements. Energy independence and environmental compatibility are two attractive features of PV systems. The fuel is free, and no noise or pollution is created from operating PV systems [1-13].

The basic solar cell usually operates at less than 1 V. Therefore, these cells are arranged in series-parallel configuration (PV module) to increase the output voltage, current and power [4]. For high voltage/power levels, the PV modules are arranged in series arrangement (PV panel), which also ensures high operating efficiency. However, such arrangements have many obstacles. A mismatch between the characteristics of the modules in the same panel always exists due to modules different orientations and/or manufacturing process. These modules, however, are restricted to conduct the same current, which limits the panel efficiency to that of least efficient module/cell. The generated current/power drops significantly, when a single cell/module is partial/fully shaded. To limit the power loss, a bypassing diode around the shaded module has to be utilized. However, all power from the shaded module is lost under these circumstances.

A proposed solution is to place a separate DC/DC converter across each PV module. The outputs of the choppers are series connected to obtain high DC voltage level. This allows the system to be transformer free, which boosts the efficiency and reduces cost, volume and weight. Furthermore, attaching a separate DC/DC chopper to each module has the advantage of decoupling the modules. This allows the maximum power point of each module to be tracked independently. Moreover, the shaded module has no impact of the remaining modules, as it could be bypassed through the DC/DC converter. Furthermore, a fault within PV module/converter disables only the faulted module/converter, while allowing the system to continue operating albeit at reduced capacity.

A little was reported about cascaded DC/DC choppers for PV applications. A simple and efficient maximum power point tracker is introduced in [5]. This Maximum Power Point Tracker (MPPT) is claimed to allow the DC/DC converters to be serially connected in the output side and operate correctly without any additional requirements, however, no detailed analysis is reported in [5] of such series connection.

Buck, boost, buck-boost and cuk DC/DC converter topologies were compared regarding steady-state efficiency in [4] for the cascaded operation. The buck-boost and cuk topologies suffer from poor switch utilization achieving of maximum of 25% at a duty cycle of 50%. Moreover, the buck-boost topology has discontinuous input/output currents, and the cuk topology has extra energy storage components. Ref. [4] concludes that buck and boost topologies are suitable for cascaded PV system; however, neither control techniques nor dynamic performance is presented in [4].

In this paper, the behavior of multi-level cascaded PV system under normal and abnormal conditions is thoroughly investigated. An innovative implementation of incremental conductance MPPT is proposed. This modified MPPT allows almost instantaneous tracking for Maximum Power Point (MPP) irrespective climatologically conditions. Therefore, each module-PV-generator-DC/DC-converter is decoupled from the remaining to achieve a fault-tolerant system.

II. TOPLOGY OF DC/DC CONVERTER

The boost and buck are most promising topologies for series connection, as claimed in [4]. The boost characteristics allow the use of minimum number of PV-generator-DC/DC-converter modules to obtain a high DC voltage level. Moreover, the input inductor reduces the ripples in the PV generator current. However, the boost topology in PV cascaded system has serious problem as shown in Fig. 1. The series connection forces equal output current, and in the boost cell $I_{in} > I_{out}$ is an operational constraint. Therefore, if a PV generator is shaded, its current drops significantly and hence the power of the entire system. To bypass the shaded PV generator, the output current has to circulate through the reverse biased PV generator, Fig. 1, which may damage the shaded module [4].

The buck topology can always track the MPP irrespective of irradiation. Moreover, in the buck based cascaded system,

each PV-generator-buck-cell is entirely decoupled from the remaining. Furthermore, in the buck cell, Fig. 1, the internal freewheel diode ensures continuous system operation under shading or fault disabling a PV generator.

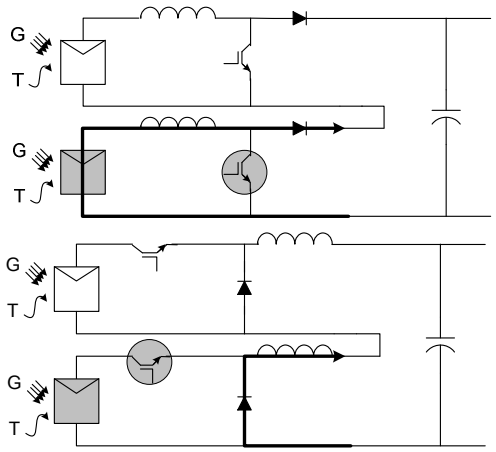

Fig. 1 Multi-level Cascaded DC/DC boost and buck converters attached to PV modules, shaded modules (grey)

III. System Architecture

The system under concern, Fig, 2, is composed of three PV generators, each coupled to a basic buck converter. Different topologies of buck converter could be used; as half-bridge. However, PV systems are unidirectional power flow; thus the basic buck topology satisfies the requirements meanwhile it simple and efficient due to reduced component count. The buck cells are in series in the output side. An independent controller for each PV generator-buck cell is used. The controller forces the PV generator to operate at their MPP independently irrespective to irradiation or other PV generators.

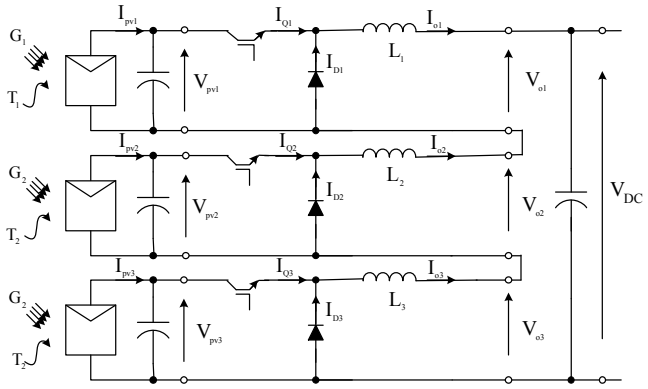

Fig. 2 Multi-level Cascaded DC/DC buck converters attached to PV generators

A detailed modeling for the different system components is given in the following.

A. PV Generator

The PV generator is modeled as a solar irradiation and temperature dependent current source I_{ph} in parallel with diode and shunt resistance R_{sh}. This combination is in series with a series resistance R_s [6].

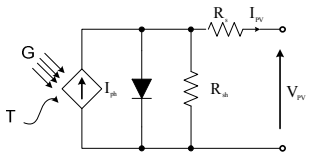

Fig. 3 Equivalent circuit of PV generator

The relation between the terminal current I_t and voltage V_t of a PV generator is expressed by,

$$I_{PV}=I_{ph}-I_o\left(e^{\frac{V_{PV}+I_{PV}R_s}{V_{th}}}-1\right)-\frac{V_{PV}+I_{PV}R_s}{R_{sh}} \quad (1)$$

Each PV generator is consisting of 20 of Kyocera KC200GT solar module. Each KC200GT module is composed of 54 series connected cell, the parameters of KC200GT module are given in Table 1 [12]. The current-voltage and power-voltage of KC200GT module calculated at 25°C and different irradiation levels are given in Figs. 4 and 5 respectively.

TABLE I
PARAMETERS OF KC200GT SOLAR MODULE AT 25°C AND 1000W²M⁻²[10]

No. of cells	54
Short circuit current	8.21A
Open circuit voltage	3.29V
Current at MPP	7.61A
Voltage at MPP	26.3V
Maximum power	200.143W
Voltage coefficient	-0.1230V/K
Current coefficient	0.0032A/K

The value of shunt resistance R_{sh} and series resistance R_s calculated by iterative method in [6] are respectively 415.405Ω and 0.221mΩ

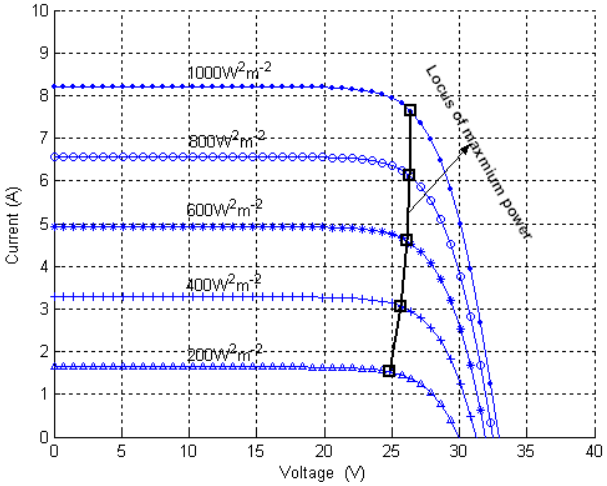

Fig. 4 Current versus voltage of KC200GT solar module at 25°C for different irradiation levels, locus of maximum power (black)

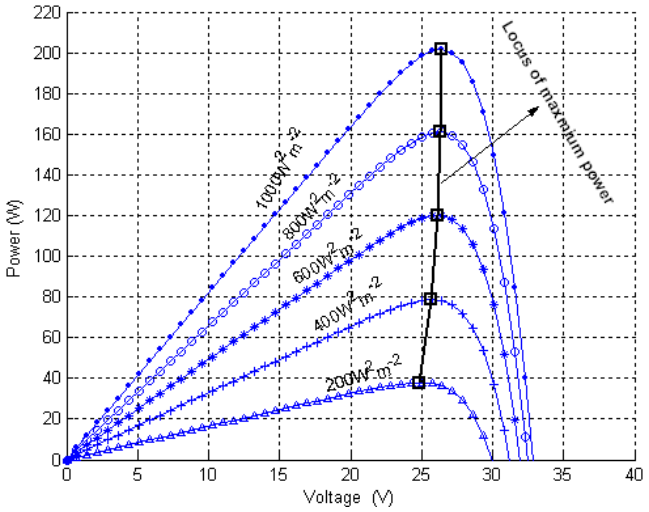

Fig. 5 Power versus voltage of KC200GT solar module at 25°C for different irradiation levels, locus of maximum power (black)

Figs. 4 and 5 reveals that the voltage at maximum power is less dependent on the solar irradiation [9].

In the series-connected system, Fig. 2, the steady-state output currents are equal $I_{o1}=I_{o2}=I_{o3}$. Assuming lossless system, the output voltage of each buck cell V_{oj} depends on ratio of cell power to that of the entire system and the DC-link voltage V_{DC}, (2),

$$V_{oj}=\frac{V_{DC}*P_{inj}}{\sum_{j=1}^{n}P_{inj}} \qquad (2)$$

The I_{ph} in (1) is generally expressed by [9],

$$I_{ph}=I_{scn}\left(\frac{G}{G_{nom}}\right)+k_i\Delta T \qquad (3)$$

where G , G_{nom}, ΔT , I_{scn} and k_i, are solar irradiance, $1000W^2m^{-2}$, temperature gradient, short-circuit current, and current-coefficient of PV generator respectively.

Equations (1)-(3) show obviously the dependency of the PV generator power on solar irradiation. Equations (1) and (3) indicate that for series-connected system, Fig. 2, when the PV generators have the same solar irradiance levels, the output powers are nearly equal, and thus the output voltages of the correspondences buck cells, (2). However, as a PV generator is partially/fully shaded, the output voltages of all buck cells are affected. The shaded module experiences reduction in the output voltage, while the unshaded modules undergo over voltage. Moreover, although the unshaded PV generators still deliver the same power, the system output current will be reduced.

B. Buck Converter

A basic buck cell is used for converter implementation. A separate inductor filter is attached to each buck cell, Fig. 2. Alternative implementation for the proposed system is using a single inductor in the DC-link. The two topologies have the same dynamic and static performance. However, the distributed inductor topology has the advantages of modularity, ease of upgrading and cost-effectiveness. Since the system can be expanded/contracted by adding/removing a buck cell with associate filter inductor.

Employing shift switching modulation strategy in the proposed system reduces the current ripple and inductor size, while maintaining high efficiency. As the switching frequency is kept constant at f_s, meanwhile the harmonics in the inductor voltage appear at $m*f_s$. Where m is the number of series converters.

The total output inductance could be calculated by [8,10],

$$L=mL_i=\frac{(V_{max}-V_{min})(1-D_{max})D_{max}}{mf_s\Delta I_o} \qquad (4)$$

where ΔI_o is ripple in the output current; D_{max}, equivalent duty cycle, where maximum ripple occurs, is equal 0.5. V_{max} and V_{min} are defined by

$$V_{max}=V_{pvi}\left(D\text{-}Dmod\frac{1}{m}+\frac{1}{m}\right) \qquad (5)$$

$$V_{min}=V_{pvi}\left(D\text{-}Dmod\frac{1}{m}\right) \qquad (6)$$

Where D is the operating duty cycle; the total inductance L computed for 5% ripple in the output current at $1000w/m^2$ solar irradiance and 25°C temperature is 0.9mH.

C. MPPT

The slope of power-voltage curve of a PV generator could be expressed by,

$$\frac{dP_{pv}}{dV_{pv}}=I_{pv}+V_{pv}\frac{dI_{pv}}{dV_{pv}}, \qquad (7)$$

The slope of power-voltage curve of a PV module, Fig. 5, is positive on the left of MPP, negative on the right and zero at MPP. Thus the relation between the incremental and instantaneous conductance is given by,

$$\begin{aligned}&\frac{\Delta I_{pv}}{\Delta V_{pv}}\succ-\frac{I_{pv}}{V_{pv}}, \text{ left MPP}\\ &\frac{\Delta I_{pv}}{\Delta V_{pv}}=-\frac{I_{pv}}{V_{pv}}, \text{ at MPP}\\ &\frac{\Delta I_{pv}}{\Delta V_{pv}}\prec-\frac{I_{pv}}{V_{pv}}, \text{ right MPP}\end{aligned} \qquad (8)$$

MPP is tracked by continuously comparing the incremental and instantaneous conductance and incrementing/decrementing the PV voltage/current. This method is reported in the literature under incremental conductance method [13].

An innovative implementation for the incremental conductance is proposed here. According to (8), the sum of the incremental and instantaneous conductance is equal to zero at MPP; therefore employing a sufficiently fast PI controller

ensures that sum is settled at zero at different operating conditions of temperature and solar irradiance.

$$E = \frac{\Delta I_{pv}}{\Delta V_{pv}} + \frac{I_{pv}}{V_{pv}}, \quad (9)$$

The bandwidth of this controller should be high enough to allow tracking for any abrupt change in solar irradiation/temperature. The controller should also provide adequate attenuation for switching ripples in the PV generator voltage and current. The merits of this control technique are simplicity, cost-effectiveness and independence on variables from other modules.

IV. Static Performance

The static performance of the proposed system is estimated through computing efficiency at different solar irradiance levels. The following assumptions are considered:

- The losses in the input and output capacitors are ignored.
- The different channels share the load equally, thus the efficiency is calculated per channel.
- The input and out filters suppress the ripples in the input and output currents

The efficiency of a channel is given by,

$$\xi = \frac{P_{inj} - P_{pv\_cu} - P_{c\_cond} - P_{c\_swit} - P_{ind\_cu}}{P_{inj}} \quad (10)$$

where P_{pv_cu}, P_{ind_cu}, P_{c_cond} and P_{c_swit} are the copper losses in the PV generators, copper losses in the output inductors conduction losses, switching losses in converter channels and respectively

The switch and the power diode in the converter channel were modeled during the on-state as a constant voltage element; thus the converter steady-state average conduction losses is given by,

$$P_{c\_cond} = V_{ce(sat)} I_{avg\_Q} + V_{on} I_{avg\_D} \quad (11)$$

Where $V_{ce(sat)}$, I_{avg_Q}, V_{on} , and I_{avg_Q} are the on-state switch drop, average switch current, diode on-state drop and diode average current respectively.

The switching frequency was determined as a compromise between the low pass filter component size and switching losses; a value of 10 kHz was chosen. The switching losses of a switch in the three converter topologies are determined from switching frequency f_s, turn on eon, and turn off e_{off} energies. The turn on e_{on} and turn off e_{off} energy curves of the proposed switches could be considered to vary linearly with the switch current, thus the switch steady-state average switching losses can be approximated by,

$$P_{c\_swit} = f_s \left(E_{on} + E_{off}\right) I_{avg\_Q} \quad (12)$$

where f_s, E_{on} and E_{off} are switching frequency, on-state constant and off-state constant respectively. substitute (11) and (12) into (10) and simplify the efficiency is given by,

$$\xi = 1 - \frac{I_{pv} R_s - V_{ce(sat)} - V_{on}\left(\frac{1}{D} - 1\right) - \frac{I_{pv}}{D^2} R_L - f_s \left(E_{on} + E_{off}\right)}{V_{pv}} \quad (13)$$

Equation (13) indicates that the efficiency depends on the operating strategy of the converter channel; and the converter drives the associated PV generator at MPP through modifying the duty cycle according to solar irradiance and temperature levels. The efficiency of the proposed cascaded PV system at different solar irradiation is illustrated in Fig. 6

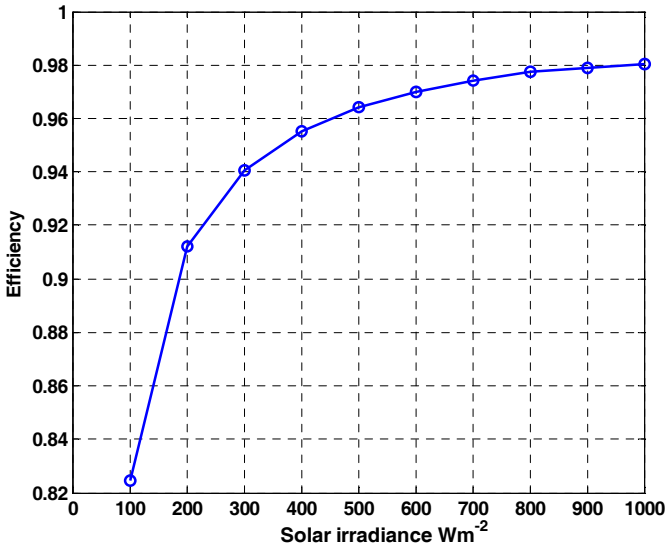

Fig. 6 Efficiency of cascaded PV system at different solar irradiation levels

Fig. 6 shows that the efficiency of the proposed system increases with the solar irradiance. The system efficiency drops significantly below 100W/m^2 insolation level. The graph illustrated in Fig. 6 shows the efficiency of the proposed system only when all modules are subjected to the same solar irradiance level. The efficiency of the proposed system is anticipated to be likely albeit lower than Fig. 6, due to the ignored losses.

V. Dyamic Response

In the following, the system performance for different climatologically conditions is investigated. The speed of MPPT convergence and the decoupling between the different channels are assessed by forcing step change in the solar irradiance in Figs. 7 and 8. This is realized by stepping the solar irradiance of generator 2 from 1000w/m^2 to 500w/m^2 at 0.1sec, 500w/m^2 to 8000w/m^2 at 0.2sec, and 8000w/m^2 to 1000w/m^2 at 0.3sec; the solar irradiance of generator 3 is stepped from 1000w/m^2 to 400w/m^2 at 0.1sec and from 400w/m^2 to 1000w/m^2 at 0.3sec. Generator 1 operates at 1000w/m^2 over the time span under concern.

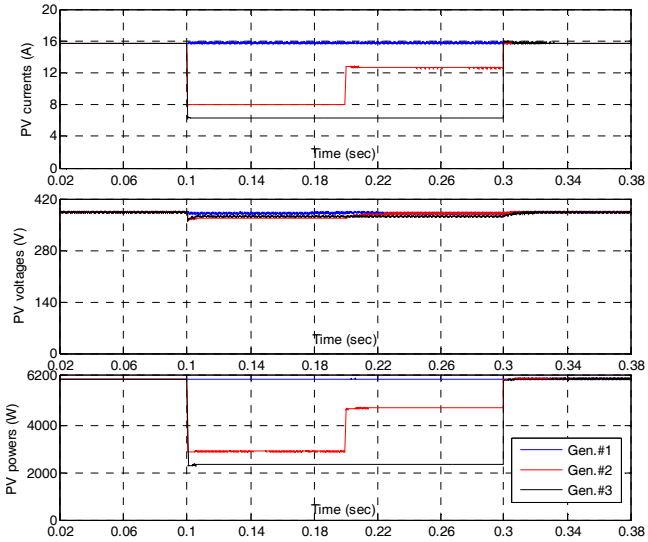

Fig. 7 Top graph: currents of PV generators, Middle graph: voltages of PV generators, Bottom graph: powers of PV generators for 25°C and 1000w/m^{2}solar irradiance for generator 1; for generator 2 solar irradiance stepped from 1000w/m^2 to 500w/m^2 at 100msec, 500w/m^2 to 8000w/m^2 at 200msec, and 8000w/m^2 to 1000w/m^2 at 300msec;for generator 3 solar irradiance stepped from 1000w/m^2 to 400w/m^2 at 100msec and from 400w/m^2 to 1000w/m^2 at 300msec

Fig. 7 shows that the PV generator currents/powers vary nearly instantaneously with the solar irradiance. The variations of the voltages of the PV generators in Fig. 7 coincide with those in Figs. 4-5. The proposed MPPT controller has the advantages of adequate tracking for MPP under abrupt changing solar irradiance and the decoupling between different PV generators. Nearly the channels have no response for conditions affecting other channels, although they shire the same DC-link.

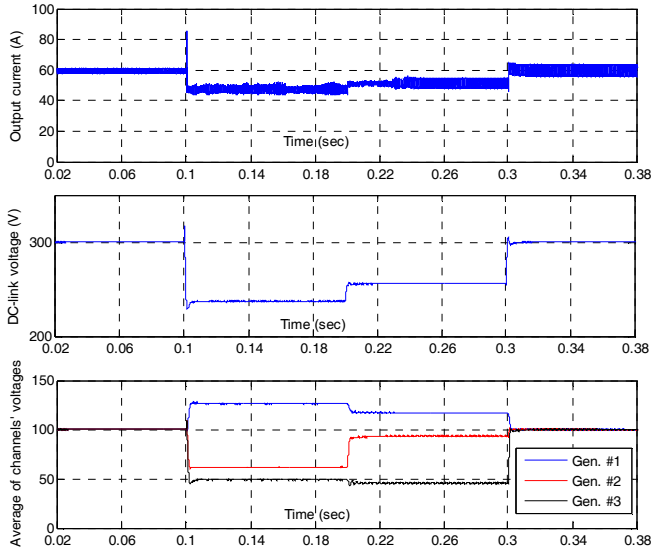

Fig. 8 Top graph: output current, Middle graph: DC-link voltage, Bottom graph average values of channels' voltages for 25°C and 1000w/m^{2}solar irradiance for generator 1; for generator 2 solar irradiance stepped from 1000w/m^2 to 500w/m^2 at 100msec, 500w/m^2 to 8000w/m^2 at 200msec, and 8000w/m^2 to 1000w/m^2 at 300msec;for generator 3 solar irradiance stepped from 1000w/m^2 to 400w/m^2 at 100msec and from 400w/m^2 to 1000w/m^2 at 300msec

The output current of the three-channels vary according to input powers/solar irradiance, Fig. 8. The shifted switching modulation strategy reduces the ripple in the output current and hence in the DC-link voltage. The spikes in the output current/voltage at 100msec are due to simultaneously change in the output powers of channel 1 and 2.

As mentioned previously that output voltage of each channel in the cascaded system depends on the channel power and the system output and DC-link voltage,(2). If a PV generator in the proposed system is subjected to lower irradiance level than those in the system, the output voltage of the shaded channel reduces, while the output voltages of the remaining changes increase. This is obvious in the bottom graph in Fig. 8. At 100msec, the solar irradiances of generator 2 and 3 are stepped from 1000w/m^2 to 500w/m^2 and 400w/m^2 respectively. The output voltages of the corresponding channels are reduced, Fig. 8, while that of channel 1 increases, which corroborates (2).

VI. System Response under Abnormal Conditions

The faults affected multi-level PV system could be in the PV generator, the DC-DC converter and the associated control circuits. The PV generators are subjected to variety of abnormal conditions such as shading, breakdown, and thermal runaway. Except the shading, the PV generators are less likely to develop abnormal condition.

The focus in this work in is on the faults in buck cell. Open and short circuit switch faults are considered here, due to their high probability and severity. These faults could be physically developed or resulted due to mal function in the gating circuit.

A. Open-circuited switch

If the switch in the buck cell develops an open circuit fault as mentioned before, the output current circulates through the freewheeling diode. Accordingly, the current of the PV generator in the faulted channel drops to zero.

Fig. 9 shows the system performance under such fault. In this Figure, PV generators 1&3 operate at 1000wm^{-2} and 25°C, while generator 2 runs at 500wm^{-2} and 25°C. Whereas, the system runs under these conditions, switch in buck cell attached to PV generator 2 encounters open circuit fault.

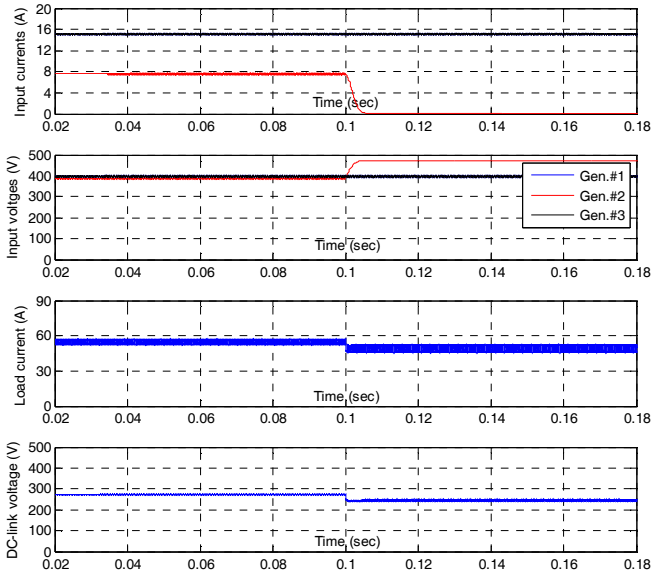

Fig. 9 Top graph: currents of PV generators, Middle top graph: voltage of PV generators, Middle bottom graph: output current (A), and Bottom graph: DC-link voltage (black) for open-circuited switch of buck converter in 2nd channel at 0.1sec. solar irradiance for PV generators 1 and 3 are 1000w/m^2 and 500w/m^2 for generator 2; all PV generators operate 25^{o}C temperature

The current and hence power of PV generator in the faulted channel ceases to zero immediately after the switch develops open-circuit fault, Fig. 8. The voltage of that PV generator rises to open circuit voltage, middle top graph in Fig. 9. The output current/voltage drops slightly, which is attributed to the loss of the power of PV generator 2. This scenario is predicted by (2).

The sustained open circuited switch has less damaging impact on the cascaded system; as the losses in PV generator in faulted channel(s) drop to zero. However, the system operates at reduced output power.

Fig. 9 shows that the unfaulty channels still operate at MPP and are not affected by the fault. This reflects the advantage of the proposed MPPT technique of decoupling the system into totally independent channels.

B. Short-circuited switch

If a switch of a buck converter in the system under concern, Fig. 2, develops a short circuit fault, the captured PV power drops to zero. The PV generator in the faulted channel operates at short-circuit point, provided that the output current is greater than the short-circuit current, $I_{sc,}$ of that generator. For this case, the current in the freewheeling diode I_D is given by,

$$I_D = I_o - I_{sc} \qquad (14)$$

If the system has output current lower than the short circuit current of the PV generator in the faulted channel, the PV generator in the faulty channel operates at ambiguous point neither open circuit or short circuit operating points. The parameters of this point are I_o and the voltage corresponding to that current. In this case, the diode current will be zero.

Fig. 10 shows the system performance under such fault.

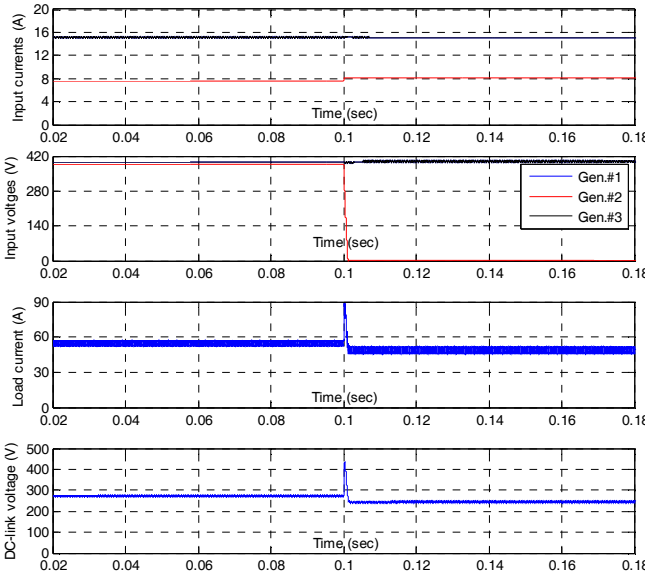

Fig. 10 Top graph: currents of PV generators, Middle top graph: voltage of PV generators, Middle bottom graph: output current (A), and Bottom graph: DC-link voltage (black) for short-circuited switch of buck converter in 2nd channel at 0.1sec. solar irradiance for PV generators 1 and 3 are 1000w/m^2 and 500w/m^2 for generator 2; all PV generators operate 25^{o}C temperature

The operation of the PV generator in the faulted channel altered from MPP pre-fault to short circuit point instantaneously during/post fault, Fig. 9. Because, the short circuit current of the generator in the faulted channel is I_{sc}=7.6A for 500w/m^2 and 25^{o}C temperature operating condition, while the load current is 55A.

Although the harvest PV power from the faulted channel for open/short circuited switch is zero; however, the sustained operation with short circuited switch stress the PV generator in the faulted channel due to elevated ohmic losses.

Again the un-faulted channels in the proposed system still are running at MPP irrespective to the status of the remaining channel, Fig. 10.

C. Open-circuited diode

If the diode of buck cell encounters open circuit, the load current has to circulate through the PV generator in the faulted channel. This may damage the generator and the buck switch, as the output current is usually greater than the generator short circuit current. This situation could be detected by monitoring the voltage drop of the buck switch during on-state. When the voltage drop of the transistor exceed that corresponding to short-circuit operating point, the controller should command the switch to permanently be opened.

D. *Short-circuited diode*

The short circuit diode fault is similar that of the switch. In both cases the captured PV power drops to zero. However for short circuited diode an extra degree of freedom is exited, that the switch could be permanently opened. This protects the corresponding PV generator from severe cupper losses.

VII. CONCLUSION

The operation of autonomous cascaded PV system under different operating scenarios was thoroughly studied; the following conclusions can be drawn:

- The boost and buck topology are most promising for cascaded system operation.
- The boost topology fails to maintain the decoupling between the channels under abnormal conditions such as partial shading.
- The system efficiency varies with the converter duty cycle, and it drops as the solar irradiance level decreases.
- The diode in the buck topology provides adequate freewheeling path for the output current in case of the corresponding PV generator is partially/fully shaded.
- Forcing the error between the incremental and instantaneous inductance to be zero, allows faster tracking for MPP.
- The short circuit switch fault encounters excessive copper losses inside the PV generator.
- The proposed cascaded system is considered to be inexpensive; moreover, the system cost is predicted to decreases in near future. This returns to the fact that PV generators have the high share in the system cost; and the continual research in PV industry may yield to reduction in the production cost of PV modules.

ACKNOWLEDGMENT

The authors are acknowledged for the Spanish Agency of International Development Cooperation (AECID) for funding this research work under A/28001/09.

REFERENCES

[1] J. T. Bialasiewicz, "Power-Electronics Systems for the Grid Integration of Renewable Energy Sources: A Survey " *IEEE Transactions on Industrial Electronics*, vol. 53, p. 1002:1016, August 2006.

[2] J. T. Bialasiewicz, "Renewable Energy System with Photovoltaic Power Generators: Operation and Modeling," *IEEE Transactions on Industrial Electronics*, vol. 55, pp. 2752-2758, July 2008.

[3] E. Endo and K. Kurokawa, "Sizing procedure for photovoltaic systems " *in IEEE First World Conference on Photovoltaic Energy Conversion*, 1994, pp. 1196 - 1199.

[4] Geofrey R. Walker and P. C. Serina, "Cascaded DC-DC Converter Connection of Photovoltiac Modules," *IEEE Transactions on Power Electronics*, vol. 19, pp. 1130-1139, 2004.

[5] A. I. Bratcu, I. Munteanu, S. Bacha, D. Picault, and B. Raison" Cascaded DC-DC Converter Photovoltaic Systems: Power Optimization Issues" *IEEE Transactions on Industrial Electronics*, vol. 19, pp. 10-17, 2010.

[6] Marcelo Gradella Villalva, Jonas Rafael Gazoli, and E. R. Filho, "Comprehensive Approach to Modeling and Simulation of Photovoltaic Arrays," *IEEE Tran. on PowerEelec.*, vol. 24, pp. 1198-1208, 2008

[7] Wu Chen, Xinbo Ruan, Hong Yan, Tse, C.K.; "DC/DC Conversion Systems Consisting of Multiple Converter Modules: Stability, Control and Experimental Verifications" *IEEE Transactions on Power Electronics*, vol. 24, pp. 1463-1474, 2005.

[8] Daniel Montesinos-Miracle, Orial Gomis-Bellmunt, Antoni Sudria-Andreu and Alfred Rufer" Multilevel DC/DC converter design for mobile applications" *PCIM 2010*, pp. 899-903, 4-6 May 2010

[9] A. A. hafez, "simple and robust Maximum Power Point Tracking Algorithm for a solar cell," *in World Congress on Electronics and Electrical Engineering (WCEEENG'10) Luxuor. Egypt, 2010,pp. 240-245,2010*.

[10] Daniel Montesinos-Miracle, Orial Gomis-Bellmunt, Antoni Sudria-Andreu and Alfred Rufer" Control of a Multilevel modular DC/DC converter design for mobile applications" *PCIM 2010*, pp. 107-110, 4-6 May 2010

[11] Marcelo Gradella Villalva, Jonas Rafael Gazoli, and E. R. Filho, "Comprehensive Approach to Modeling and Simulation of Photovoltaic Arrays," *IEEE Transactions on power electronics*, vol. 24, pp. 1198-1208, 2009.

[12] "KC200GT High Efficiency Multicrystal Photovoltaic Module Datasheet Kyocera : http://www.kyocera.com.sg/products/solar/pdf/kc200gt.pdf. 2011"

[13] T. Esram, P. L. Chapman " Comparison of Photovoltaic Array Maximum Power Point Tracking Techniques" *IEEE Transactions on Energy Conversion*, vol. 22, 2007.